Digital Radiometers for Earth Science

Christopher Ruf and Steven Gross

Space Physics Research Laboratory, University of Michigan, Ann Arbor, MI 48109-2143

***Abstract* — Digital microwave radiometers replace as much of the conventional analog circuitry in a radiometer as possible with an analog-to-digital converter followed by a high speed Digital Signal Processing (DSP) stage. Digital technology adds capabilities to a radiometer that would otherwise be much more difficult (and often cost prohibitive) to include. The quality of each of the performance enhancements enabled by digital radiometry (*e.g.* spectral resolution, RFI detectability threshold, and full Stokes polarization purity) is dependent on certain aspects of the digital technology (e.g. number of bits of digitization, digitization oversampling rate, length of transverse digital filters, number of internal bits utilized by the DSP algorithm, and core memory and logic block sizes in the DSP chip). These factors are examined and current and projected radiometer performance capabilities estimated given the current and projected state of the art in DSP technology.**

***Index Terms* — Radiometer, Digital signal processing.**

I. Introduction

Digital radiometers replace as much of the conventional analog circuitry as possible with an Analog-to-Digital Converter (ADC) followed by a high speed Digital Signal Processing (DSP) stage. The conversion to digital technology improves the long term stability and independence from temperature variations of the radiometer, thus improving and simplifying its calibration. Digital technology can also add capabilities to a radiometer that would be much more difficult (and often cost prohibitive) to include otherwise. The signal bandwidth can be digitally subdivided into many well isolated sub bands. This simplifies the removal of RFI, which tends to have a highly localized spectrum. The DSP stage can also be programmed to detect other moments of the signal amplitude, in addition to the second moment that is detected by a conventional analog square-law detector diode. In particular, the second and fourth central moments have been shown to be an extremely sensitive detector of RFI [3, 6, 7]. Thus, digital radiometers are much more capable than analog designs of both detecting and removing RFI from the observations. If a radiometer operates with two orthogonal linear polarization channels, then the DSP stage can also be used to perform a complex correlation between the two polarizations, in addition to the conventional self-correlation. This results in a fully polarimetric radiometer (including 3rd and 4th Stokes brightness temperatures) for little additional cost or complexity over that of a two polarization analog design. Fully polarimetric radiometers can be useful in two ways. They allow for the retrieval of additional geophysical information related to the partial coherence between orthogonal linear polarization signals. The retrieval of near surface wind direction over the ocean is one example of this [1, 2, 8]. A fully polarimetric radiometer is also able to more accurately compensate for leakage between polarization channels and, thus, produce more accurately calibrated measurements of the conventional vertical and horizontal linear polarization brightness temperatures [4, 5].

II. Space Based Correlators

A. Overview

Recent technology developments with space-based cross-correlators for Fourier synthesis interferometers have been driven by several proposed Earth Science remote sensing missions – in particular the Lightweight Rainfall Radiometer (LRR) and the Geosynchronous Earth Orbit Synthetic Thinned Aperture Radiometer (GEOSTAR). In both cases, emphasis has been placed on reducing the power requirements, increasing the clock speed, and improving the radiation tolerance of the digitizers and the multipliers/accumulators through the use of ultra-low power CMOS ASICs based on a 0.5 V logic protocol with resistance by design to radiation-induced single event upsets. This protocol has extensive spaceflight heritage for other high speed digital signal processing applications in space, and it has been adapted to Earth science needs in support of the LRR and GEOSTAR missions.

B. Current Technology

Ultra-low power 0.5 V CMOS 2-bit digitizer ASICs were fabricated in ~2002 for the LRR program that required 5.5 mW while sampling at ~220 MHz. The maximum sample rate was 300 MHz, at which rate the DC power draw rose to 9.5 mW. An ultra-low power 0.5 V CMOS 2-bit 25 channel complex multiplier/accumulator ASIC was also developed for LRR at this time. It included a front end digital quadrature demodulation stage to form the In Phase and Quadrature Phase components of the input signal, followed by complex multipliers and accumulators for all possible pairs of the 25 complex signals. When clocked at ~220 MHz, the chip drew 1.5 W. Both of these ASICs were built using 250 nm design rules.

A reduction in design rules for the ultra-low power 0.5 V CMOS process, from 250 nm to 90 nm, has been accomplished since 2002 as a result of other, non-correlator, spaceflight digital signal processing projects. Because of

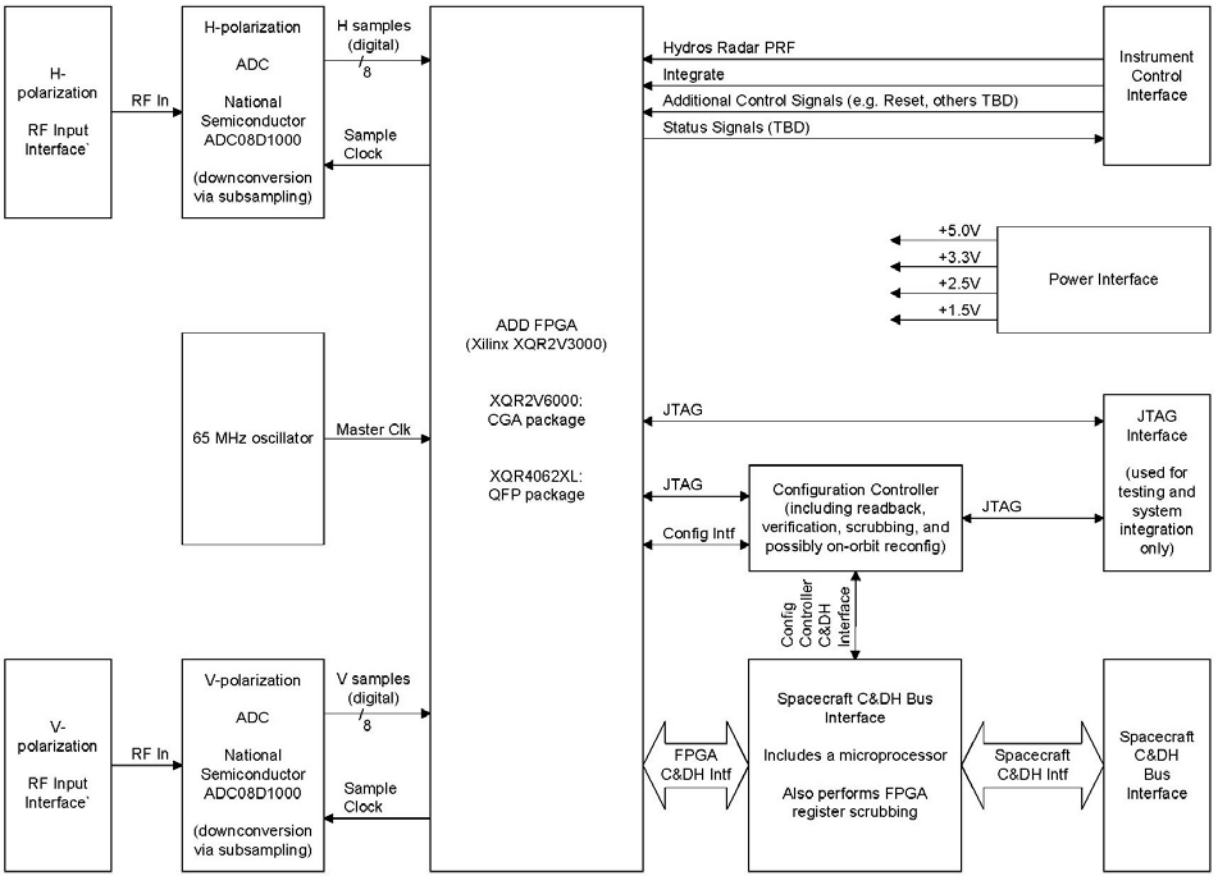

Fig. 1. Functional block diagram of the SMAP Digital Back End. SMAP has been recommended by the recent NRC Decadal Survey. It will use digital radiometer technology in order to mitigate the effects of RFI and enable fully polarimetric (four Stokes) measurements for minimal added complexity or cost in mass, power or size.

these developments, it is possible to significantly improve upon the earlier LRR ASIC performance. A new ASIC development effort is currently funded to create a new multiplier/accumulator ASIC for the GEOSTAR project using the 90 nm geometry. It is projected to be capable of complex cross-correlations of all possible pairs of 196 In Phase and 196 Quadrature Phase 2-bit input signals, clocked at 1400 MHz, while drawing 1.68 W of DC power.

C. Future Technology and Recommendations

Further reductions in the power required of, and further increases in the maximum clock rates supported by, the ultra-low power 0.5 V CMOS ASICS will be possible as the design rules decrease further in size. Preliminary developments are underway at 65 nm for other, non Earth science, applications and are expected to continue. These developments should eventually mature to the point where they can be leveraged for our application. An acceleration in that development process would require additional infusion of funds. Leveraging of the current 90 nm process for the development of faster and/or lower power digitizers than those developed for LRR has lagged behind that for the multiplier/accumulator chips. In order to maintain a reasonably close match between the maximum clock rate capabilities of the digitizers and multipliers/accumulators, it is recommended that additional development funds be considered for the digitizers. In particular, development is recommended of 90 nm versions of the LRR-style digitizers. Based on the modeling projections made for the 90 nm multiplier/accumulator ASICs, this can be expected to result in digitizers with maximum clock rates in the neighborhood of 1400 MHz. By comparison, current flight qualified digitizers capable of ~2 GHz clock rates require ~2 W of power to operate. The power needed is much too high to be supportable for typical large-N interferometer systems. A 90 nm ultra-low power 0.5 CMOS ASIC digitizer can be expected to reduce the power required by ~ two orders of magnitude. Utilization of even narrower design rules (65 nm or lower) will produce even better performance.

III. Example of Field Deployed Radiometer

A digital radiometer back end has been developed as a proof of concept demonstration for the NASA SMAP mission. It consists of two 8-bit ADCs (one each for the vertical and horizontally polarized channels) clocked at 65 MHz, followed by a field programmable gate array (FPGA) to implement the


(a)

(b)

(c)

(d)

Fig. 2. Field campaigns conducted as part of a current IIP project to move the technology required for the SMAP mission to TRL-6. (a) Truck mounted deployment near an air traffic control radar; (b) Ground based integration with the NASA/JPL PALS prototype for SMAP; (c) Ground based integration with the NASA DSN system for radio astronomical studies of non-thermal emission by Mars; and (d) airborne deployment on the NASA WB-57 with the NOAA/ETL PSR instrument.

DSP stage. The DSP algorithm begins with 16 digital filters, which divide the input spectrum into sub bands of 1.5 MHz bandwidth each. For each sub band, the first four moments of the voltage amplitude are calculated. This allows for RFI to be reliably detected and removed. Complex correlations are also performed between each of the v- and h-pol sub bands, from which the fully polarimetric Stokes brightness temperatures can be derived. A functional block diagram of the SMAP digital back end is shown in Fig. 1. Prototypes of the SMAP system have been operated in four field campaigns to date as part of the progression of the technology readiness of the design to TRL 6 [6, 7]. The campaigns included ground based and truck mounted deployments with L-Band radiometers, a ground based deployment with an X-band radio telescope, and an airborne deployment on the NASA WB-57 with the NOAA/ETL PSR instrument, as illustrated in Fig. 2. These field campaigns have successfully demonstrated, in a relevant environment, the principle advantages of a digital radiometer in terms of the added performance capabilities.

IV. Conclusions

Digital radiometers used for Earth science applications have been demonstrated in laboratory, and ground and airborne field campaigns. Current commercial technology is capable of meeting most if not all of the science user needs. However, significant technology development is still required to meet the current and expected future needs of spaceborne users. These needs include lower power operation, faster maximum clock rates, and lower radiation susceptibility.

References

[1] Bettenhausen, M.H., C.K. Smith, R.M. Bevilacqua, N.-Y. Wang, P.W. Gaiser and S. Cox (2006). "A nonlinear optimization algorithm for WindSat wind vector retrievals," IEEE Trans. Geosci. Remote Sens., 44(3), 597-610.

[2] Brown, S.T., C.S. Ruf and D.R. Lyzenga (2006). "An Emissivity Based Wind Vector Retrieval Algorithm for the WindSat Polarimetric Radiometer," IEEE Trans. Geosci. Remote Sens., 44(3), 611-621.

[3] De Roo, R., S. Misra and C. Ruf (2007). "Sensitivity of the Kurtosis Statistic as a Detector of Pulsed Sinusoidal RFI," IEEE Trans. Geosci. Remote Sens., 45(7), 1938-1946.

[4] Gasiewski, A.J., and D.B. Kunkee (1993). "Calibration and applications of polarization correlating radiometers, "IEEE Trans. Microwave Theory Tech., 41(5), 767-773.

[5] Njoku, E.G., E.J. Christensen and R.E. Cofield (1977). "The SeaSat scanning multichannel microwave radiometer (SMMR):

Antenna pattern correction development and implementation," IEEE J. Oceanic Eng., 5(2), 125-137.

[6] Ruf, C.S., S. M. Gross and S. Misra (2006a). "RFI Detection and Mitigation for Microwave Radiometry with an Agile Digital Detector," IEEE Trans. Geosci. Remote Sens.,44(3), 694-706.

[7] Ruf, C., S. Misra, S. Gross and R. De Roo (2006b). "Detection of RFI by its Amplitude Probability Distribution," Proc. 2006 IEEE International Geoscience and Remote Sensing Symposium, Denver, CO.

[8] Yueh, S.H., W.J. Wilson, S.J. Dinardo and S.V. Hsiao (2006). "Polarimetric microwave wind radiometer model function and retrieval testing for WindSat," IEEE Trans. Geosci. Remote Sens., 44(3), 597-610.